Supplementary Information for:

Tuning the vertical location of helical surface states in topological insulator heterostructures via dual-proximity effects

Guangfen Wu[1,2], Hua Chen[3,4], Yan Sun[5], Xiaoguang Li[6,3,1], Ping Cui[1,3], Cesare Franchini[5], Jinlan Wang[2], Xing-Qiu Chen[5], and Zhenyu Zhang[1,7,4]

[1]*ICQD, Hefei National Laboratory for Physical Sciences at the Microscale, University of Science and Technology of China, Hefei, Anhui, 230026, China*

[2]*Department of Physics, Southeast University, Nanjing, 211189, China*

[3]*Department of Physics and Astronomy, University of Tennessee, Knoxville, TN 37996, USA*

[4]*Department of Physics, University of Texas, Austin, TX 78712, USA*

[5]*Shenyang National Laboratory for Materials Science, Institute of Metal Research, Chinese Academy of Sciences, Shenyang, 110016, China*

[6]*State Key Laboratory of Surface Physics and Department of Physics, Fudan University, Shanghai, 200433, China*

[7]*School of Applied Science and Engineering, Harvard University, Cambridge, MA 02138, USA*

S1. Key properties of the Zn*M* (*M* = S, Se, Te) conventional insulators (CIs)

In this section we give a systematic comparison of the band gap, the spin-orbit coupling (SOC) strength, and the work function of Zn*M* under different conditions (strain and dimensionality).

For bulk semiconductors, the SOC strength is defined as $\Delta_{SO} = \varepsilon\left(\Gamma_{8v}\right) - \varepsilon\left(\Gamma_{7v}\right)$ at the top of the valence band, according to Ref. 1 (see Supplementary Fig. 1a for the case of bulk ZnTe). For the single-layered Zn*M* films, we use the magnitude of the SOC-splitted gaps in the valence band as a measure of the SOC, as shown in Supplementary Figs. 1b-f. In Supplementary Fig. 2 we also show the strength of SOC defined in an alternative way: the difference in band gap with and without SOC, $\Delta_{SO}^{'} = V_g(noSOC) - V_g(SOC)$. Both definitions give the same trend for the bulk Zn*M*, i.e., SOC is increasing in the sequence of ZnS-ZnSe-ZnTe, agreeing well with experiments[2] as depicted in the left panel of Supplementary Fig. 2. For the single-layered Zn*M* under different strains due to epitaxy on the TI substrates (see Table I in the main text), the overall trend of the SOC is the same as that in the bulk, but with reduced magnitudes (right panel of Supplementary Fig. 2).

The band gaps of bulk Zn*M* are smaller by about 50% compared with the experimental values[2] due to the fact that the generalized gradient approximation usually underestimates band gaps. However, the trend that the band gap is decreasing in the sequence of ZnS-ZnSe-ZnTe is correctly reproduced by our calculations, as shown in the left panel of Supplementary Fig. 2. In the right panel of Supplementary Fig. 2 we show the band gaps for the single-layered Zn*M*. In particular, we calculated the band gaps of single-layered ZnTe with compressive (-3.9%), zero, and tensile

strains (+1.6%), and the trend suggests that the band gap will decrease as the strain goes from compressive to tensile. As a final note, the work function of the single-layered ZnTe film also sensitively depends on strain (Table I in the main text), which increases as the strain goes from compressive to tensile.

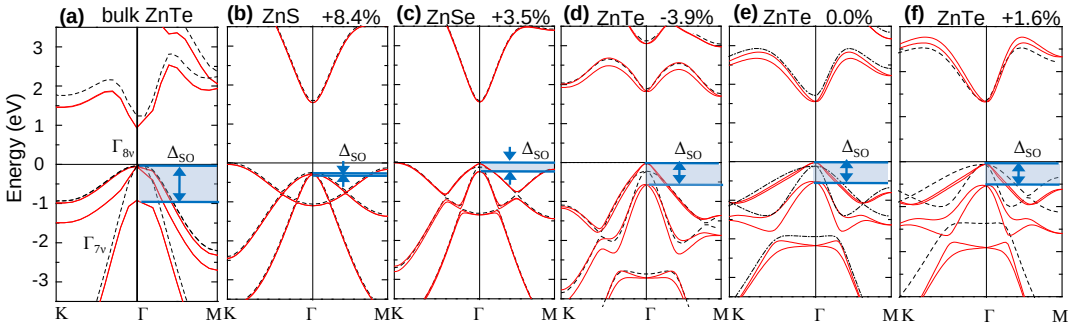

Supplementary Figure 1 | Band structures and SOC-induced gaps of bulk ZnTe and differently strained single-layered Zn*M* (*M* = S, Se, Te). a, Bulk ZnTe. **b**, ZnS with a tensile strain of +8.4%. **c**, ZnSe with a tensile strain of +3.5%. **d-f**, ZnTe with strain of -3.9%, 0.0%, and +1.6%, respectively. The red solid and black dashed curves correspond to the band structure with and without SOC, respectively.

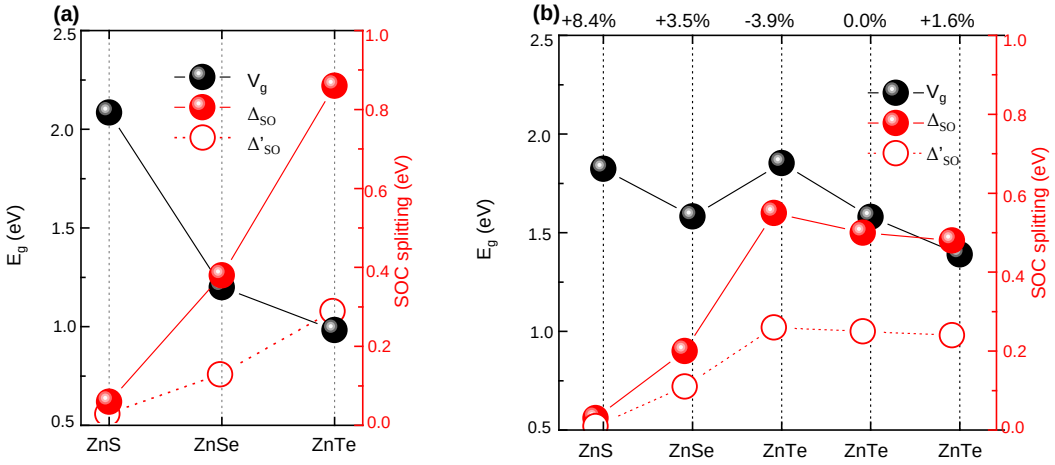

Supplementary Figure 2 | Band gap and SOC splitting of Zn*M* (*M* = S, Se, Te). a, bulk Zn*M*. **b**, single-layered Zn*M* (M = S, Se, Te) with different strains: +8.4% for ZnS, +3.5% for ZnSe, -3.9%, 0.0%, and +1.6% for ZnTe.

S2. Band structures of the Bi_2Se_3 and Bi_2Te_3 substrates.

The inclusion of SOC in our calculations closes the band gap through introducing a single Dirac-cone at the Γ point, which is the topological surface state (TSS), for both the 6QL Bi_2Se_3 and 6QL Bi_2Te_3 slabs[3], as shown in Supplementary Fig. 3. For the corresponding 1QL slabs, the energy gaps persist, despite significantly reduced, after the inclusion of the SOC, which is due to the coupling of the TSSs from the two surfaces.

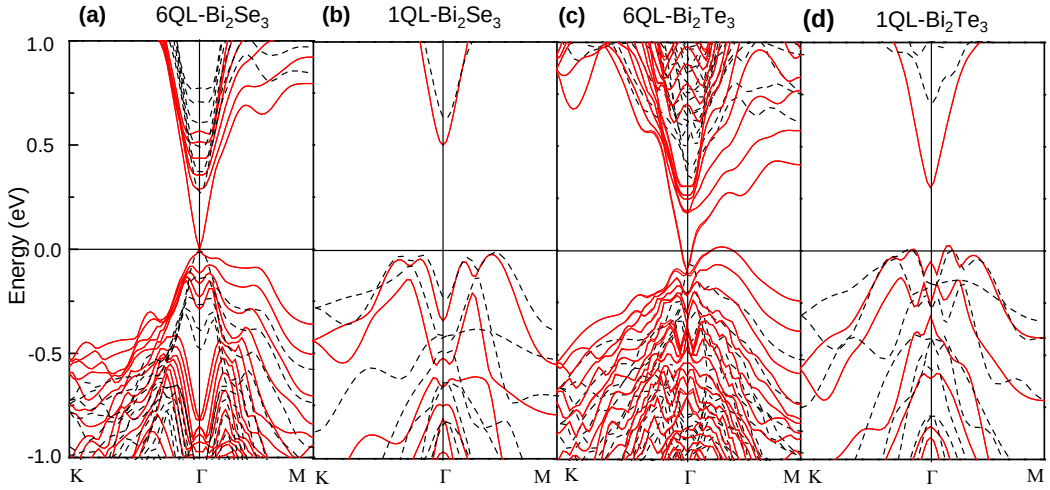

Supplementary Figure 3 | Band structures of Bi_2Se_3 and Bi_2Te_3. a, 6QL-Bi_2Se_3. **b**, 1QL-Bi_2Se_3. **c**, 6QL-Bi_2Te_3. **d**, 1QL-Bi_2Te_3. The red solid and black dashed curves correspond to band structures with and without SOC, respectively.

S3. Band structures of the Bi_2Se_3 substrate and the ZnSe/Bi_2Se_3 heterostructure with varied SOC strengths.

To see the correlation between the SOC strength and the topological properties of the systems, we have tuned the SOC strength, λ_{SO}, in both the Bi_2Se_3 substrate and ZnSe/Bi_2Se_3 heterostructure. Here λ_{SO} is the term used in the Hamiltonian of the system from the contribution of the SOC, while Δ_{SO} defined in the main manuscript is the SOC-split gap in the valence band as a measure of the SOC effect. For Bi_2Se_3, the use of substantially smaller values of λ_{SO} than that in the actual material system would fail to close the bulk band gap, thereby giving no TSS (Supplementary Figs. 4a-b), while the use of a too strong SOC would severely distort the bulk valence bands, thereby destroying the TSS as well (Supplementary Fig. 4d). For ZnSe/Bi_2Se_3, as we

reduce the λ_{SO} of the entire system, TSS will again disappear, as it depends on the bulk topology (Supplementary Fig. 5).

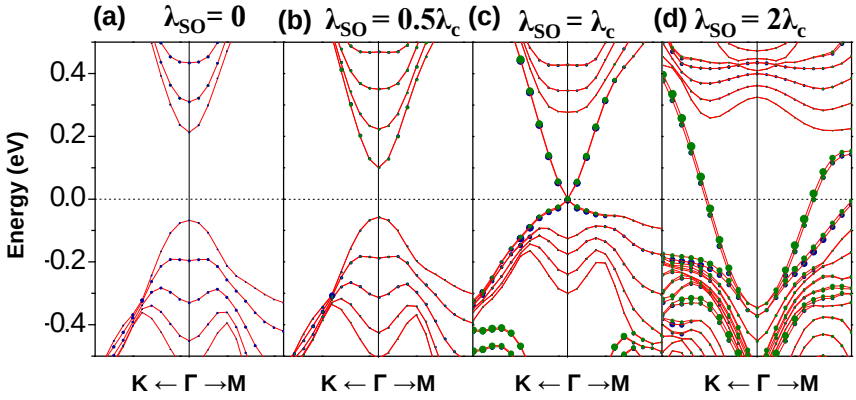

Supplementary Figure 4 | Band structures of Bi_2Se_3 with different SOC strengths (λ_{SO}) along the K← Γ →M direction. The green and blue dots indicate the electronic bands contributed by the 1st and 6th QL of the Bi_2Se_3, respectively; the size of the dots indicates different spectral weights. λ_{SO} is the SOC strength we exploited, while λ_c is the SOC strength in the actual physical systems.

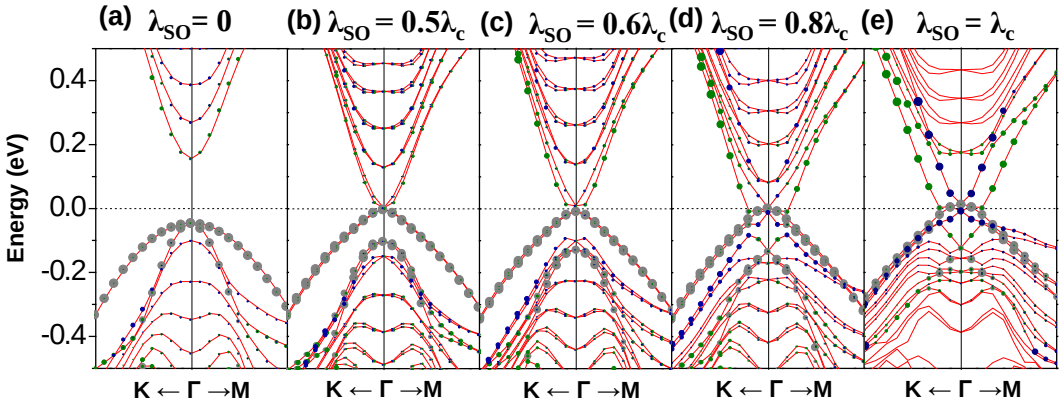

Supplementary Figure 5 | Band structures of $ZnSe/Bi_2Se_3$ with different SOC strengths (λ_{SO}) along the K← Γ →M direction. The grey, green and blue dots

indicate the electronic bands contributed by the ZnSe overlayer, the 1st and 6th QL of the Bi_2Se_3, respectively. All other symbols are the same as in Supplementary Fig. 4.

References

1. Cardona, M. *in Solid State Physics*, edited by Seitz, F., Turnbull, D., & Ehrenreich, E. (Academic, New York, 1969), Vol. 11.

2. Adachi, S. *Properties of Group-IV, III–V and II–VI Semiconductors* (John Wiley & Sons Ltd, Chicheste, 2005).

3. Zhang, H. *et al.* Topological insulators in Bi_2Se_3, Bi_2Te_3 and Sb_2Te_3 with a single Dirac cone on the surface. *Nature Phys.* **5,** 438-442 (2009).